

Improvement in Retinal Blood Vessel Detection Using Modified Time-Frequency Analysis Algorithms for Ophthalmic Disease Diagnosis

AkramAsghari Govar^{1*}, Ali Baibourdiaghdam

Department of Electrical Engineering, AharBranch, Islamic Azad University, Ahar, Iran

Department of Biomedical Engineering, AharBranch, Islamic Azad University, Ahar, Iran

Email: AK-Asghari@iau.ac.ir (corresponding author)

Receive Date: 23Jul 2025 Revise Date: --- Accept Date: 19Aug 2025

Abstract

In medical image processing, there are significant challenges related to image clutter, uneven intensity distribution, and image blurring when extracting blood vessels. Therefore, finding an appropriate method for optimal preprocessing, noise removal, and image enhancement, as well as identifying effective filters and segmentation techniques for blood vessels, is essential. Addressing these issues can greatly assist ophthalmologists in achieving faster and easier segmentation of retinal blood vessels, thereby improving diagnostic accuracy. Therefore, accurate extraction of the retinal blood vessel tree is used for screening, eye diseases, and the diagnosis of complications resulting from cardiovascular diseases. For this purpose, a new method is employed to extract vessel centers, utilizing an improved Philopator combined with the application of small-sized circular structural elements. After enhancing the retinal blood vessels, the fuzzy clustering technique, specifically the C-means algorithm, is applied to estimate the actual width of the vessels. Finally, by combining the results obtained from the two stages—vessel center extraction and fuzzy clustering—the final segmentation of the blood vessels is achieved. The performance of the proposed improved algorithm has been evaluated in terms of accuracy, sensitivity, and specificity on the DRIVE and STARE datasets, and the obtained data has been analyzed. Finally, a comparison between the proposed algorithm and previous methods has been carried out, with their strengths and weaknesses analyzed and presented.

Keywords: retinal vessels, eye diseases, Tophat operator, fuzzy clustering algorithm, image processing

1.Introduction

Physical illnesses such as diabetes, cataracts, cardiovascular diseases, hypertension, and others can cause changes in the retina. When the blood vessels in the retina are damaged, they may leak fluid or blood, leading to swelling of the retinal tissue or the formation of deposits called "exudates." This damage can also result in the growth of fragile, tangled blood vessel branches that can destroy the retina. If left untreated, these issues can lead to severe vision loss or blindness. To this end, retinal vessel segmentation algorithms are considered. In this context, artificial

neural networks have been extensively studied for feature extraction from the eye retina, such as vessel features. According to the study by N. Dey, et al. proposed an algorithm for extracting retinal vessels, in which they enhanced the vessels using the CLAHE preprocessing method and then extracted the retinal vessels using a fuzzy clustering technique [1]. In 2013, Mr. F. M. Villalobos-Castaldi and colleagues utilized local entropy information combined with the Gray-Level Co-occurrence Matrix (GLCM) for vessel segmentation. First, a homogenous filter was applied to enhance the vessels by

calculating the GLCM, which is considered a statistical feature. Then, local entropy thresholding was used for retinal vessel segmentation, resulting in high accuracy for extracting the vessels [2]. M. G. Cinsdikici et al proposed a hybrid model combining a homogenous filter and an ant colony algorithm for retinal vessel segmentation. After the preprocessing step, the image is processed simultaneously using the homogenous filter and the ant colony algorithm. The results are combined using length filtering to achieve complete vessel extraction. This algorithm was tested on retinal images from the DRIVE database, and the optimal parameters were determined. However, it incorrectly identifies damaged areas as vessels, and the segmented vessels appear thicker compared to those in the gold standard images [3]. B. Sumathy et al proposed an automatic segmentation method for extracting retinal vessels, in which morphological opening was used for preprocessing to remove the vessel center reflections, and an averaging filter was applied to reduce background estimation and noise in the green channel images of the retina. Then, the Tophat operation was used to enhance vessel visibility in the images, and finally, an entropy-based thresholding technique was employed for the retinal vessel segmentation step [4]. A unique technique for detecting the centerlines of vessels was proposed by M. M. Fraz and colleagues. In this method, the vessel centerlines are extracted using the first derivative of the Gaussian filter in four directions, followed by evaluating the signs of the obtained values and calculating their average. Then, mathematical morphological Tophat

filtering with a linear structuring element is applied to obtain the entire network of vessels, with the final images being combined to form the complete retinal vessel network [5]. In another study referenced in [6], the clarity of the retinal images was first improved using the CLAHE operator, and then a suitable background estimation was achieved by applying a morphological closing operation with two different sizes. Subsequently, a binary image of the segmented vessels was obtained by applying a threshold. B. Dai et al initially extracted the centers of the vessels by employing a set of directional line detectors. Using similarity criteria and adaptable matching strategies, a complete vascular network was obtained with an associated threshold value [7]. The authors improved the Dijkstra algorithm by utilizing the generation of morphological operators to extract vessel intersection points and accurately determine the optimal parameters for energy minimization [8]. In a recent study, Asahgri and colleagues combined image processing techniques, Gabor filters, and proposed using a sharpening method to eliminate noise and enhance image clarity. This approach provided a better visualization of retinal vessels for subsequent processing stages. They further suggested an improved method for background estimation and removal, as well as employing a morphological reconstruction algorithm to restore the vascular structure, ultimately leading to the final segmentation of retinal vessels [9].

2. Tophat and bottom-hat transforms

The combination of image subtraction with opening and closing operations results in transformations called Tophat and bottom-hat. One of the main applications of these transformations is in removing objects from an image using a structuring element during opening or closing operations. This occurs when the size of the structuring element does not match the size of the object in the image. Then, the difference operation creates an image in which only the removed

components remain. The Tophat transform is used for bright objects on a dark background, while the bottom-hat transform is applied for the opposite case. An important application of the Tophat transforms is in correcting the effects of uneven illumination. Proper or uniform lighting plays a crucial role in object extraction from the background. This process, known as segmentation, is one of the key steps in automatic image analysis [10-12].

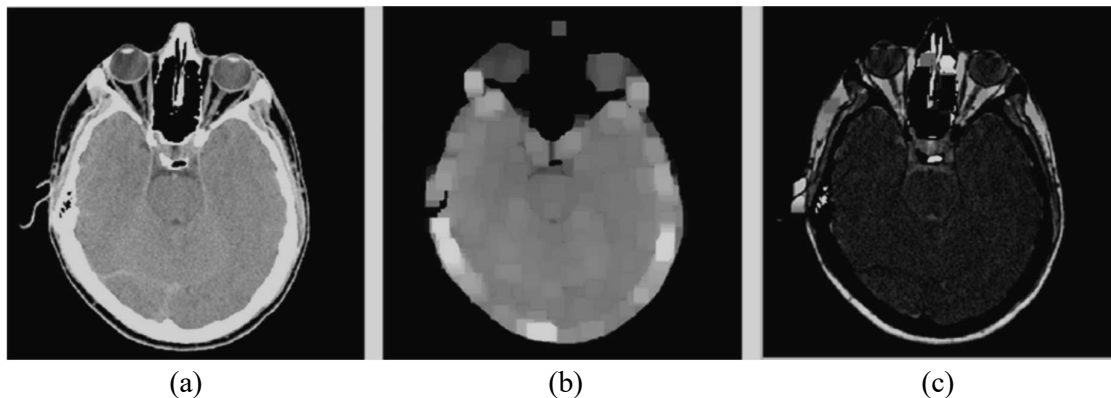


Fig. 1. a) Original image b) Applying the morphological opening operation c) Applying the Tophat morphological transform

As observed, the Tophat operator can be used in image processing for segmentation and edge detection of image components.

3. Local filters

Techniques in the spatial domain are applied directly to the image pixels. Implementing some methods in the spatial domain is easier and more meaningful. Generally, spatial domain techniques are computationally more efficient and require fewer processing resources. Spatial filters are often used to enhance the display of image features. The term "filter" is derived from frequency domain processing, where "filtering" refers to passing or rejecting

certain frequency components. For example, a low-pass filter allows low frequencies to pass. The effect produced by low-pass filters is blurring or smoothing of the image. Using spatial filtering, this can be done directly on the image. Linear smoothing filters are used for blurring or noise reduction. Blurring is usually employed in the preprocessing stage.

4. Fuzzy C-Means clustering algorithm

It is a well-known algorithm for pattern recognition issues. This algorithm operates based on fuzzy pixel classification. In this clustering technique, each pixel is assigned to multiple classes with membership

degrees, which are values between 0 and 1. In this algorithm, the cluster centers are calculated by minimizing a dissimilarity function, using an iterative process. By updating the cluster centers and the membership degrees of each pixel to these centers, the centers gradually move to their correct positions within the set of pixels belonging to each cluster. The operation of the fuzzy C-means algorithm is as follows. Initially, the membership matrix $U = [u_{ij}]$ is assigned random values for each pixel of the image according to the following relation. In fact, u_{ij} determines the degree or value of the membership function for each pixel i in cluster x_i .

$$\sum_{i=1}^c u_{ij} = 1 \quad \forall \quad j = 1, 2, \dots, n \quad (1)$$

The performance index PI for the membership matrix U and centers C_i is calculated using the following relation.

$$J(U, C_1, \dots, C_c) = \sum_{i=1}^c J_i = \sum_{i=1}^c \sum_{j=1}^n u_{ij}^m d_{ij}^2 \quad (2)$$

In the above relation, u_{ij} represents a value between 0 and 1, serving as the membership function for pixel ij , and c_i refers to the center of the i^{th} cluster. Furthermore, d_{ij} denotes the Euclidean distance between the i^{th} cluster center and the j^{th} data point. The parameter m is a weighting balance that ranges from 1 to infinity. In order to reach the minimum value of the dissimilarity function, the following two conditions must be satisfied.

$$C_i = \frac{\sum_{j=1}^n u_{ij}^m x_j}{\sum_{j=1}^n u_{ij}^m} \quad (3)$$

$$u_{ij} = \frac{1}{\sum_{k=1}^c \left(\frac{d_{ij}}{d_{ki}} \right)^{\frac{2}{m-1}}} \quad (4)$$

The fuzzy C-means algorithm consists of the following four steps:

1. The membership matrix U is randomly initialized using relation 1.
2. The centers are determined using relation 2.
3. The dissimilarity between centers is calculated using relation 3. If this value is less than a pre-defined threshold, the algorithm terminates.
4. A new membership matrix U is computed from the membership values using relation 4, and the algorithm returns to step 2 [13].

5. The Suggested Algorithm

In this paper, an algorithm is proposed that enhances the desirable features of the previous algorithm described in [9]. The goal is to improve the algorithm's ability to accurately detect both thin and thick retinal vessels. Studying the pixel values of the vessels in retinal images indicates that these pixels have uncertain or ambiguous values. Detecting these pixels, particularly the thin retinal vessels, is challenging. In many cases, the pixel values of the background and the vessels are very close, making segmentation more difficult. In such conditions, we hypothesize that fuzzy methods can contribute significantly to improving retinal vessel detection. To this end, by making modifications to the approach in [9] and incorporating a fuzzy stage, the segmentation results on retinal images have been analyzed. This has led to the development of a new algorithm designed for more accurate segmentation of retinal vessels. This algorithm also consists

of three main phases. The first phase is preprocessing, which is implemented similarly to that in [9]. The second phase is the processing stage, which includes two steps: the extraction of vessel center points and the fuzzy segmentation of retinal vessels in the images. The third phase concerns post-processing, where the results obtained from the two processing steps are combined to produce the final segmented images. The innovations of the proposed algorithm are summarized as follows:

- Utilization of an improved normalized morphological operator using structural elements of varying sizes for the vessel center extraction and fuzzy segmentation stages.
- Introduction of a new idea to enhance retinal vessels during the processing stage, achieved by combining three image processing techniques: histogram range, CAHE (Contrast Adaptive Histogram Equalization), and the median filter.

5.1. Preprocessing phase

The goal at this stage is to obtain a complete region of both thin and thick retinal blood vessels. This phase consists of two steps: 1) extracting the centers of the vessels, which is aimed at accurately detecting the thin vessels. 2) fuzzy segmentation of the retinal vessels, which is performed to determine the actual width of the thick vessels. For extracting the vessel centers, an improved Ball-Cohen method using a small structuring element has been employed. The reason for using this morphological operator with a small structuring element size is due to the expected dependence of the morphological filter responses on the vessel width. Since the width of thin and thick blood vessels in

retinal images varies, choosing a small structuring element ensures that only the pixels with a size smaller than the structuring element remain unchanged in the image, while the intensity values of other pixels are reduced. In the improved Tophat operator, the closing operation is used to estimate background fluctuations, and the opening operation is applied to remove the vessels. The Tophat operator is obtained from the following relation.

$$T_{hat}(I) = I - (I \circ S_o) \quad (5)$$

In this relation, S_o is the structuring element of the opening operator.

When the opening operator is applied to an image, all pixel intensities in the resulting image remain less than or equal to the pixel intensity values of the original image. Since the background of retinal images contains small-sized and scattered noise points, this causes the difference between the image obtained by applying the opening operator and the original image to introduce minor fluctuations in the image. To prevent this issue, we first add a step of applying the closing operator before performing the opening operator in the Tophat algorithm. Then, a minimum operation is performed between the resulting image and the original image. This ensures that the final image matches the original image at all points except at the peaks and valleys. Next, the resulting image is subtracted from the original image to reveal the retinal vessels, while other areas become fully smoothed. The improved Tophat operator is defined by relation 6.

$$TopHat_I = I - \min(I \bullet S_c) \circ S_o; I \quad (6)$$

In the above formula S_c refers to the structuring element of the closing operator, and S_o refers to the structuring element of

the opening operator. Fig.2, part (a), shows the standard Tophat operator. As observed, after applying the opening operator to the initial image, which is marked by red circles, the pixel intensity values decrease up to the vicinity of the circular structuring element. In areas of the image that contain small-width noise, the space between pixels extends to the circle's environment because the opening structuring element does not reach the surface of those pixels. Fig.2, part (c), shows the improved Tophat operator. In this figure, first, the closing operation, indicated by the yellow color, removes the image noise. After that, the opening operation is applied to the image, which removes the vessel-related peaks. Then, a minimum operation is performed between the resulting image and the original image. The background images obtained from the standard Tophat and the improved Tophat operators are respectively shown in parts (b) and (d) of Fig.2. One noteworthy point here is that using the improved Tophat

operator with a large-sized structuring element can only reveal the thick vessels in retinal images, with thinnest vessels being eliminated. Conversely, the improved Tophat operator with a small-sized structuring element helps to reveal the fine blood vessels of the retina, although the actual width of the thick vessels is lost. Therefore, in the step of extracting vessel centers, the focus has been on extracting fine vessels, and for this purpose, the improved Tophat operator with a small structuring element has been used to reveal the vessel centers, especially the thin vessels in retinal images. To this end, the size of the closing structuring element was chosen as 1, and the size of the opening structuring element was chosen as 2.

The result of applying the proposed filter, the improved Tophat operator with a small-sized structuring element, is shown in Fig.3.

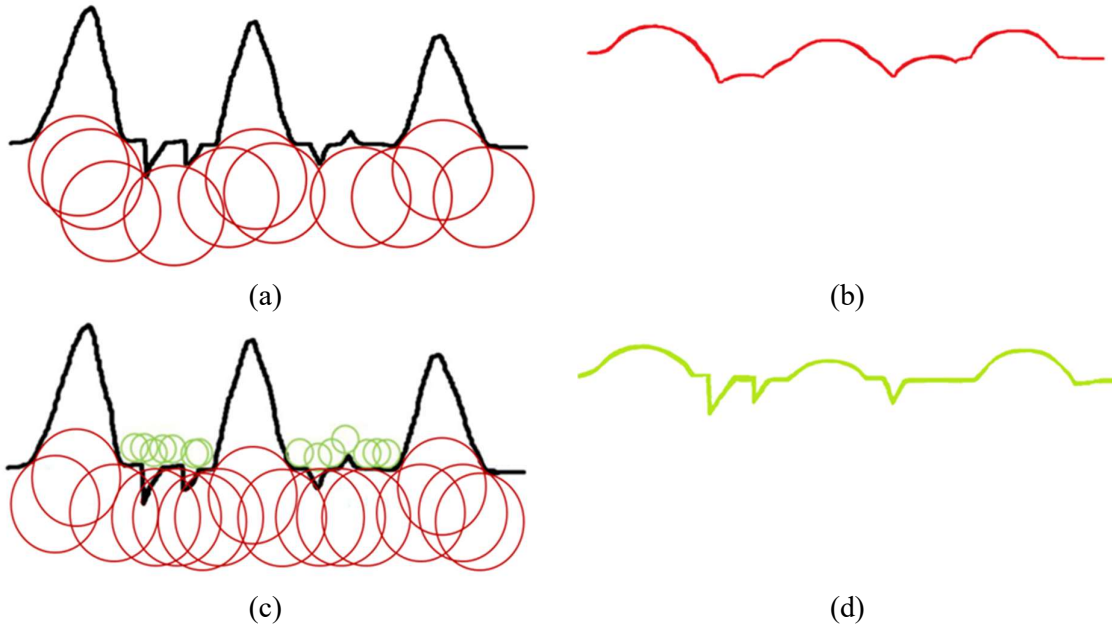


Fig.2. (a) Standard Tophat operator, (b) Background estimation using the standard Tophat operator, (c) Improved Tophat operator, (d) Background estimation using the improved Tophat operator

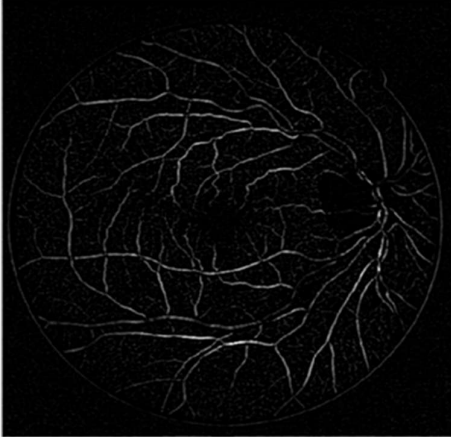


Fig.3. Image of vessel centers after applying the proposed filter, the improved Tophat operator with a small-sized structuring element

After applying the improved Tophat operator with a small-sized structuring element, a binary image is obtained from

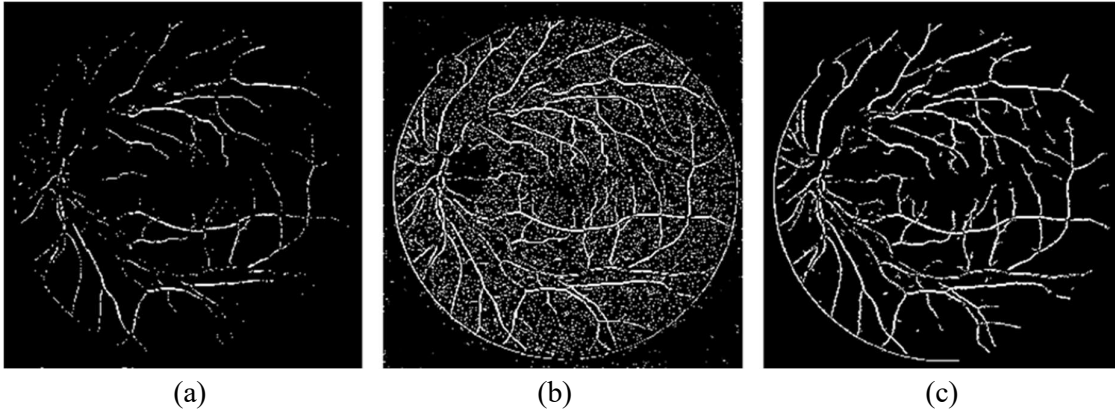


Fig.4. Vessel centers after reconstruction: (a) Marker image, (b) Mask image, (c) Reconstructed image

As previously mentioned, using a small-sized structuring element is not effective in correctly identifying thick vessels in images. To address this issue and obtain the true width of retinal vessels, in the fuzzy segmentation stage, a large structuring element Tophat operator is initially used to obtain an image containing thick vessels. In this stage, the size of the closing structuring element is considered as 1, and the size of the opening structuring element as 10. Then, the intensity values related to the identified

the resulting image using a morphological recognition operator. The marker and mask images are generated using thresholding methods. The marker image results from applying a large threshold value, while the mask image results from applying a small threshold value. The reconstruction operator allows for obtaining a binary image with the maximum number of thin vessels and minimal noise points in the image. The result of using this technique is shown in Fig.4. Part (a) of Fig.4 displays the marker image. Part (b) shows the mask image, and part (c) presents the result of the morphological reconstruction.

vessels are amplified as follows. For this purpose, a combination of three effective image processing techniques is proposed. First, based on the histogram of the image, a range is found that displays only the vessels in the image. Then, the intensities of all pixels within this range are doubled. Fig.5. (a) The image obtained by applying the improved Tophat operator with a large structuring element. (b) The image resulting from the enhancement of retinal vessels.

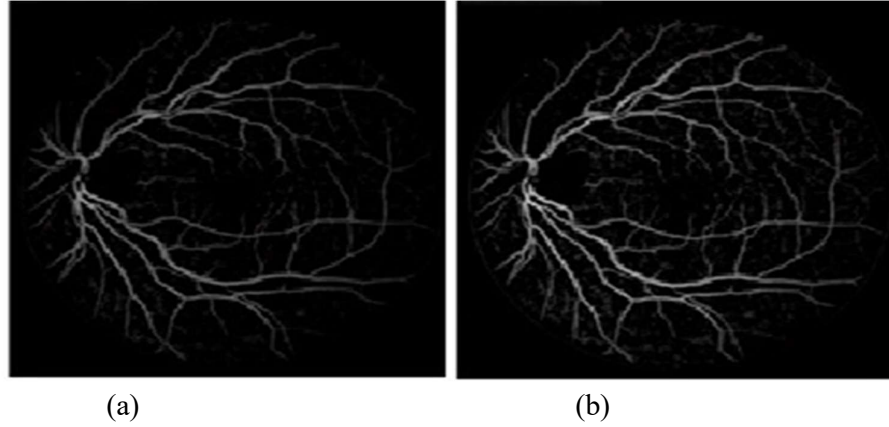


Fig.5. (a) Vessel image after applying the improved Tophat filter with a large-sized structuring element. (b) Vessel enhancement using the vessel histogram.

Then, the CLAHE technique is applied to the image to further improve the vessel clarity. Next, a median filter with a large size of 60 is used to remove the remaining noise from the image, and the final image is obtained by subtracting this processed image from the previous step. This process facilitates the detection of vessels during

the subsequent fuzzy clustering C-means stage. Fig.6 shows, in part (a), the vessel image after applying the CLAHE filter; part (b) displays the background image; and part (c) shows the result of subtracting the background image from the image in part (a).

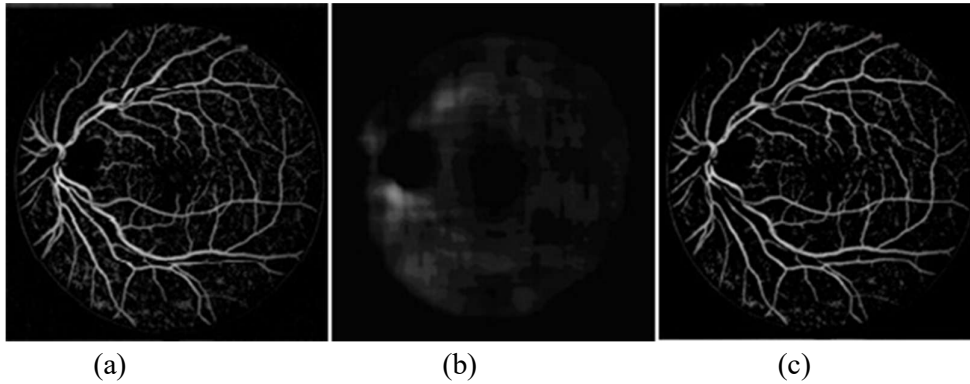


Fig.6. (a) Vessel image after applying the CLAHE filter; (b) Noise estimation of the image using the median filter; (c) Enhanced image.

Then, the fuzzy algorithm is applied to the obtained image. After the vessel pixels with their actual width are identified in the image resulting from the fuzzy segmentation steps, the process proceeds to the next stage of the algorithm. The resulting image is shown in Fig.7.



Fig.7. Image obtained from the fuzzy clustering algorithm.

5.2. Post-processing phase

In the post-processing stage, the two binary images obtained from the vessel center extraction and fuzzy segmentation steps are combined. The final image, after removing the circle around the eye, consists of a suitable binary image containing both thin and thick vessels in the retinal images, which is shown in Fig.8.

5.3. Samples of the final segmentation images

Samples of the final segmentation results by the proposed algorithm are shown on

the DRIVE and STARE databases, respectively, in Figs.9 and 10.

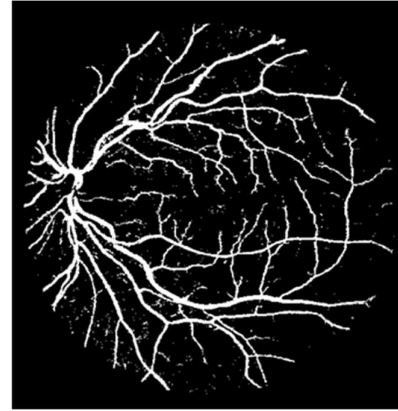
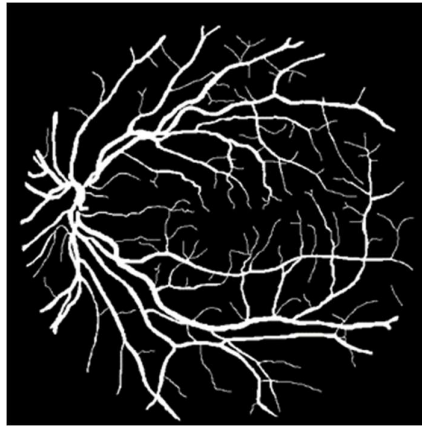
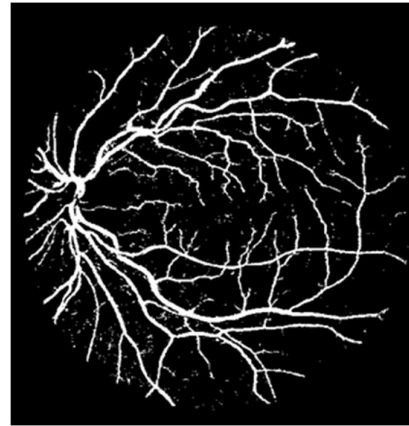


Fig.8. Final vessel image after combining the results

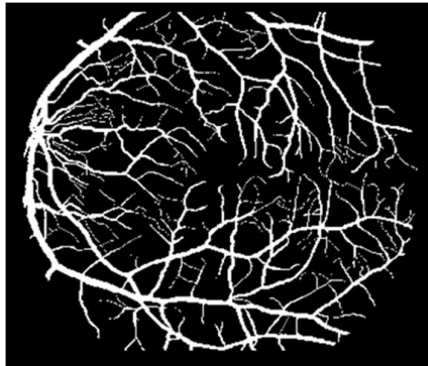


(a)

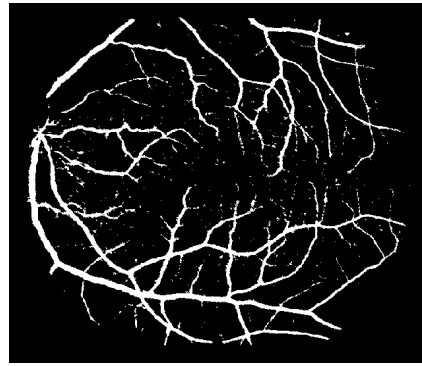


(b)

Fig.9. sample images DRIVE, a) standard image, b) image segmented by the proposed algorithm



(a)



(b)

Fig.10. sample images STARE, a) standard image, b) image segmented by the proposed algorithm

Tables 1 and 2 compare the proposed algorithms with other methods for segmenting retinal blood vessels.

Considering that the ultimate goal is to improve precision, sensitivity, and feature values for the evaluation metrics, the

proposed methods are compared with each other as well as with other techniques mentioned in the table.

Table1. The values obtained from the implementation of the proposed algorithm for the DRIVE database

method	accuracy	sensitivity	specificity
proposed method	95.05	78.03	96.70
Asghari[9]	95.21	74	97.26
Ricci [2]	95.63	-	-
Osareh [14]	95.24	96.14	94.84
Lili Xu[15]	93.28	77.60	-
N Dey[1]	95.03	99.62	54.66
Fraz [5]	95.79	75.02	85.97
B Dai[7]	94.60	70.91	98.06
Lupascu [18]	95.97	-	-
Li [20]	-	78.00	80.97

Table 2. Comparison of the proposed algorithm with previous methods described in the articles on the STARE database.

method	accuracy	sensitivity	specificity
proposed method	95.05	73.69	96.82
Asghari[9]	95.11	73.37	96.88
Ricci[2]	95.84	-	-
DMarin [16]	95.26	69.44	98.19
Salem[17]	-	82.15	97.50
Fraz[5]	94.42	73.11	96.80
Li[20]	-	75.20	98.00
Lam[19]	96.14	-	-

6. Conclusion

The proposed algorithm has achieved a higher sensitivity value compared to the algorithm in reference [9]. This advantage is due to the use of a fuzzy approach in the

proposed algorithm as well as the application of morphological processing techniques based on pattern recognition of blood vessels in retinal images. Additionally, the proposed algorithm has obtained satisfactory results in terms of accuracy and feature metrics, with only slight differences compared to the algorithm in reference [9]. Furthermore, the comparison of the proposed algorithm with other methods demonstrates its superior performance relative to several techniques presented in the literature. Moreover, taking into account the desirable values of the evaluation metrics, the proposed algorithm has achieved a suitable segmentation of retinal blood vessels with only a small difference less than some other methods listed in the comparison table.

References

- [1] Dey, N., A. B. Roy, M. Pal, and A. Das. "FCM Based Blood Vessel Segmentation Method for Retinal Images." arXiv preprint arXiv:1209.1181, 2012.
- [2] Villalobos-Castaldi, F. M., E. M. Felipe-Riverón, and L. P. Sánchez-Fernández. "A Fast, Efficient and Automated Method to Extract Vessels from Fundus Images." *Journal of Visualization*, vol. 13, 2010, pp. 263–270.
- [3] Ricci, E., and R. Perfetti. "Retinal Blood Vessel Segmentation Using Line Operators and Support Vector Classification." *IEEE Transactions on Medical Imaging*, vol. 26, 2007, pp. 1357–1365.
- [4] Cinsdikici, M. G., and D. Aydın. "Detection of Blood Vessels in Ophthalmoscope Images Using MF/Ant (Matched Filter/Ant Colony) Algorithm." *Computer Methods and Programs in Biomedicine*, vol. 96, 2009, pp. 85–95.
- [5] Sumathy, B., and S. Poornachandra. "Retinal Blood Vessel Segmentation Using Morphological Structuring Element and Entropy Thresholding." *Proceedings of the Third International Conference on Computing*

- Communication & Networking Technologies (ICCCNT), 2012, pp. 1–5.
- [6] Fraz, M. M., et al. "An Approach to Localize the Retinal Blood Vessels Using Bit Planes and Centerline Detection." *Computer Methods and Programs in Biomedicine*, vol. 108, 2012, pp. 600–616.
- [7] Joshi, Shilpa, and P. T. Karule. "Retinal Blood Vessel Segmentation." *International Journal of Engineering and Innovative Technology (IJEIT)*, vol. 1, no. 3, 2012, pp. 175–178.
- [8] Dai, B., W. Bu, X. Wu, and Y. Teng. "Retinal Vessel Segmentation via Iterative Geodesic Time Transform." *Proceedings of the 21st International Conference on Pattern Recognition (ICPR)*, 2012, pp. 561–564.
- [9] Espona, L., M. J. Carreira, M. Penedo, and M. Ortega. "Retinal Vessel Tree Segmentation Using a Deformable Contour Model." *Proceedings of the 19th International Conference on Pattern Recognition (ICPR)*, 2008, pp. 1–4.
- [10] Asghari Govar, A., and A. Baibourdi Aghdam. "Using Modified Time-Frequency Algorithms for Retinal Vessel Detection to Diagnose Eye Diseases." *Journal of Artificial Intelligence in Electrical Engineering*, in press.
- [11] Roushdy, M. "Comparative Study of Edge Detection Algorithms Applying on the Grayscale Noisy Image Using Morphological Filter." *GVIP Journal*, vol. 6, 2006, pp. 17–23.
- [12] Gonzalez, R. C., and R. E. Woods. *Digital Image Processing*. Prentice Hall, 2002.
- [13] Gasparri, J., A. Bouchet, G. Abras, V. Ballarin, and J. Pastore. "Medical Image Segmentation Using the HSI Color Space and Fuzzy Mathematical Morphology." *Journal of Physics: Conference Series*, 2011, p. 012033.
- [14] Sopharak, A., B. Uyyanonvara, and S. Barman. "Automatic Exudate Detection from Non-Dilated Diabetic Retinopathy Retinal Images Using Fuzzy C-Means Clustering." *Sensors*, vol. 9, 2009, pp. 2148–2161.
- [15] Osareh, A., and B. Shadgar. "Automatic Blood Vessel Segmentation in Color Images of Retina." *Iranian Journal of Science and Technology, Transactions B: Engineering*, vol. 33, 2009, pp. 191–206.
- [16] Xu, L., and S. Luo. "A Novel Method for Blood Vessel Detection from Retinal Images." *Biomedical Engineering Online*, vol. 9, 2010, p. 14.
- [17] Marín, D., A. Aquino, M. E. Gegúndez-Arias, and J. M. Bravo. "A New Supervised Method for Blood Vessel Segmentation in Retinal Images by Using Gray-Level and Moment Invariants-Based Features." *IEEE Transactions on Medical Imaging*, vol. 30, 2011, pp. 146–158.
- [18] Salem, S. A., N. M. Salem, and A. K. Nandi. "Segmentation of Retinal Blood Vessels Using a Novel Clustering Algorithm (RACAL) with a Partial Supervision Strategy." *Medical & Biological Engineering & Computing*, vol. 45, 2007, pp. 261–273.
- [19] Lupascu, C. A., D. Tegolo, and E. Trucco. "FABC: Retinal Vessel Segmentation Using AdaBoost." *IEEE Transactions on Information Technology in Biomedicine*, vol. 14, 2010, pp. 1267–1274.
- [20] Lam, B. S. Y., Yongsheng G., and A. W. C. Liew. "General Retinal Vessel Segmentation Using Regularization-Based Multiconcavity Modeling." *IEEE Transactions on Medical Imaging*, vol. 29, 2010, pp. 1369–1381.
- [21] Li, W., A. Bhalerao, and R. Wilson. "Analysis of Retinal Vasculature Using a Multiresolution Hermite Model." *IEEE Transactions on Medical Imaging*, vol. 26, 2007, pp. 137–152.